# Morphologies and Electrical Properties of Electrospun Poly[(*R*)-3-hydroxybutyrate-*co*-(*R*)-3-hydroxyvalerate]/ Multiwalled Carbon Nanotubes Fibers

**Kok Ho Kent Chan,[1] Siew Yee Wong,[2] Wuiwui Chauhari Tiju,[2] Xu Li,[2] Masaya Kotaki,[1] Chao Bin He[2]**

[1]*Department of Advanced Fibro-Science, Kyoto Institute of Technology, Sakyo-Ku, Kyoto 606-8585, Japan*
[2]*Institute of Materials Research and Engineering, A*STAR (Agency for Science, Technology and Research), 3 Research Link, Singapore 117602, Singapore*

Received 11 June 2009; accepted 24 September 2009
DOI 10.1002/app.31572
Published online 17 December 2009 in Wiley InterScience (www.interscience.wiley.com).

**ABSTRACT:** Electrospinning process was used to fabricate fine fibers from poly[(*R*)-3-hydroxybutyrate-*co*-(*R*)-3-hydroxyvalerate] embedded with multiwalled carbon nanotubes (MWCNTs). Rotating disc collector was used to provide additional drawing force to stretch and align both the embedded MWCNTs and electrospun fibers themselves. Morphological observation revealed MWCNTs aligned to the fiber axis and protruding from the surface. To understand the electrical properties of the fiber, a single-composite fiber has been deposited on a substrate, across multiple electrodes. Electrical conductivity of the single-electrospun fiber with low MWCNT content of 0.2 wt % was calculated to be in a remarkable magnitude of about 2.07 $Sm^{-1}$. Electrical current flow spanning the fiber length of 1400 μm indicates that the presence of an interconnected network of MWCNTs exists within the fiber. © 2009 Wiley Periodicals, Inc. J Appl Polym Sci 116: 1030–1035, 2010

**Key words:** electrospinning; multiwalled carbon nanotubes; morphology; electrical conductivity; disc collector

## INTRODUCTION

Electrospinning is an efficient fiber fabrication technique, which uses a high-voltage electric field to generate polymeric solution jets from a fine nozzle. During spinning, cone-like solution droplet is developed at the nozzle, in which a flow of polymeric fluid is continuously drained into the pointed tip, to form the ejected solution jets. These jets solidify to form fine fibers upon removal of the residing solvents.[1–4] Although the setup for electrospinning is relatively simple, it has been demonstrated that via the use of rotating disc or stationary plate collector, the process is capable of fabricating continuous yarns, fibrous mats composed of uniaxially[5] and randomly orientated fine nanofibers.

To functionalize and improve the physical properties of fibers, several authors have suggested the fabrication of electrospun composite micron and nanofibers incorporated with carbon nanotubes (CNTs).[6–24] The motivations in using CNT composite systems are derived from the exploitation of the nanotubes' intrinsic advantages, and it has been demonstrated that the introduction of CNTs into polymers can provide improved mechanical properties and both electrical and thermal conductivities.[6–11] In addition, the nature of CNT structure enables their surfaces to be modified chemically with various functional groups, as demonstrated by a handful of research groups.[12–14] Past studies have also highlighted that addition of CNTs can increase crystallinities and change crystal morphologies of the polymer matrix.[15–17]

Now, the use of CNT-filled biopolymer composites has generated remarkable interest in the field of tissue engineering and biomedical applications. Considerable efforts have been made to understand and evaluate the interaction between CNTs and living mammalian cells.[13,18,19] To exploit the biological advantages associated with the CNT-filled biopolymer composite system for medical applications, this study focuses on the fabrication of electrospun multiwalled CNT (MWCNT)-filled poly[(*R*)-3-hydroxybutyrate-*co*-(*R*)-3-hydroxyvalerate] (PHBV) composite fibers.

Another attractive characteristics of processing CNT composite system via electrospinning lie in the anticipation that the CNTs within the polymeric solution would align and disperse themselves along the fiber axis during the spinning process, as suggested by Dror et al.[20] Because of the fine diameters

*Correspondence to:* X. Li (x-li@imre.a-star.edu.sg), M. Kotaki (m-kotaki@kit.ac.jp) or C. B. He (cb-he@imre.a-star.edu.sg)

of electrospun fibers, it has been observed that some of the embedded CNTs would be dispersed and exposed on the surfaces of the fibers.[20,21] In the case of tissue engineering, it is still unclear whether the direct contact of cultivated cells with CNTs would be harmful; but there are several reported cases of cells being cultivated directly on CNTs, and these articles have demonstrated positive outcomes in cell proliferation.[12,13,22] With respect to electrical properties, Ojha et al.[23] highlighted that high concentration of CNTs on fiber surfaces is advantageous for conductance; as such morphology encourages conduction paths to be established between multiple fibers, as in the case of fiber mat.

In this work, biocompatible polymer, PHBV solution dispersed with nitric acid surface-treated MWCNT was electrospun on both stationary plate and rotating disc collector. The stretching force provided by the rotating disc was expected to reduce fiber diameters and further encourage the dispersion and alignment of MWCNTs within the fibers.[24] Morphology and dispersion state of MWCNTs within the fibers were observed using scanning electron microscope (SEM) and transmission electron microscope (TEM), respectively. To understand the effect of MWCNTs on the structural properties and development of crystal phases within electrospun PHBV/MWCNT composite fibers, FTIR spectroscopy analysis was performed on electrospun fibers collected on stationary plate collector. Current–voltage measurements were performed on a single-composite fiber with low content of MWCNT to investigate the electrical properties of the composite system. Using two probes placed on electrodes in contact with different sections of the fiber, this work has successfully derived the conductivity of the fiber, after taking into consideration the contact resistance involved in the system.

## EXPERIMENTAL

### Materials

Natural source poly[(*R*)-3-hydroxybutyrate-*co*-(*R*)-3-hydroxyvalerate] (PHBV) with hydroxyvalerate (HV) content of 8 wt % ($M_w$ 600,000, $M_w/M_n = 3.7$) was purchased from Aldrich (USA) and purified by dissolving in chloroform followed by filtration and subsequent precipitation in hexane. Hexane, chloroform, and 1,2-dichloroethane were supplied by Aldrich.

To prepare PHBV solution for electrospinning, the purified polymer was dissolved in mixed solvent of chloroform and 1,2-dichloroethane (2/3; v/v) at 12 wt %. The mixture was then stirred at 50°C overnight to encourage complete dissolution. The PHBV/MWCNT solution for electrospinning was prepared by dissolving PHBV and acid-treated MWCNTs (Cheap Tubes, Inc, Brattleboro, VT) in mixed solvent of chloroform and 1,2-dichloroethane (2/3; v/v) at 17 wt % via ultrasonification. MWCNT composition was changed from 0.2 to 0.8 wt %. Acid treatment of MWCNT was carried out according to the previously reported approach.[25]

### Electrospinning setup

The basic apparatus for electrospinning includes a high-voltage power supply, a fine capillary, and a grounded collector. The electrostatic force generated ejects the polymer solution droplet at the tip of the capillary into a jet, which eventually deposits as fibers onto the collector.

Randomly oriented and aligned fibers were fabricated via electrospinning, using a static plate and rotating disc collector respectively. The rotational velocity of the disc collector was varied at 750 and 1500 rpm, which correspond to 470 and 940 m/min in take-up velocity, respectively. For all the experiments, electrospinning had been carried out at an applied voltage of 12 kV using 22 gauge size needle (about 0.4 mm inner diameter opening) with a needle-to-collector distance of 150 mm.

### Characterization method

SEM (JEOL JSM-5600) was used to observe the morphologies of electrospun pure PHBV and PHBV/MWCNT composite fibers. TEM (JEOL 2000) had been used to examine the dispersion of MWCNT within the fibers. Fiber diameters had been measured using software ImageJ. Bruker Equinox 55 Fourier transform infrared spectrometer was used to analyze the molecular vibrations of electrospun fiber mats.

To prepare the fiber for electrical characterization, a single-electrospun PHBV/MWCNT (0.2 wt %) fiber was isolated and deposited onto an indium phosphate substrate with gold electrodes deposited on it. The gold electrodes were spaced about 200 μm apart, and each electrode was about 200 μm wide. The instrument used for electrical measurement is a two-probe system, HP4140B Semiconductor parameter analyzer. Current–voltage characteristics were obtained by fixing one of the probes on a single point along the fiber, pressing it against the gold electrode, while shifting the other probe and placing it on different points on the fiber. The probes were adjusted to press the fiber tightly onto the gold electrode. A potential difference from −5 to 5 V was provided between the two probes, and the output current was recorded. In the derivation of contact resistance value, fiber segments between the two probes in contact with the gold electrodes are assumed to be highly conductive and thus not taken into consideration in calculation. Fiber diameters and lengths were measured using ImageJ program via SEM micrographs scaling.

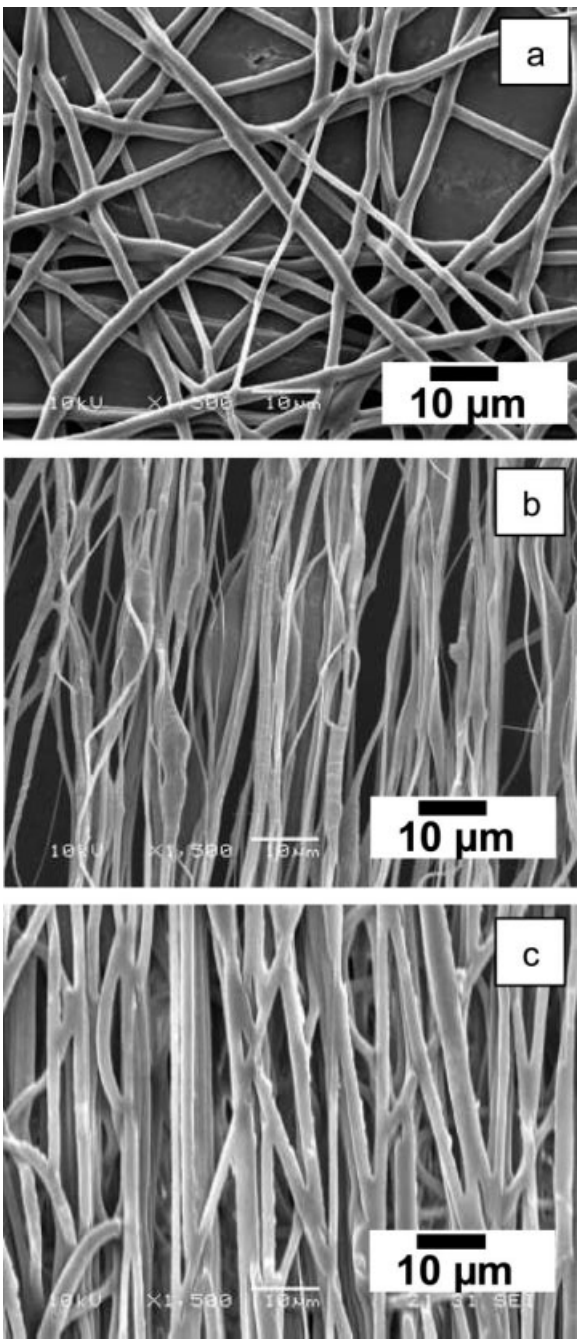


**Figure 1** SEM images showing electrospun PHBV/MWCNT (0.2 wt %) fibers collected on (a) stationary plate collector, (b) rotating disc collector at take-up velocity of 470 m/min, and (c) electrospun PHBV fibers collected using disc collector at take-up velocity of 470 m/min. Magnification for all the images is the same.

## RESULTS AND DISCUSSION

### Morphology of electrospun PHBV/MWCNT fibers

Figure 1(a) shows the SEM image of randomly oriented electrospun PHBV/MWCNT fibers, obtained using static plate collector. The fibers were electrospun from PHBV-based composite with 0.2 wt % MWCNT dissolved in the chloroform and 1,2-dichloroethane. Average fiber diameter was calculated to be 1.8 ± 0.6 μm. Figure 1(b) shows the SEM image for the aligned electrospun composite fibers with MWCNT of 0.2 wt %, obtained from the edge of a disc collector. The fibers were collected at a take-up velocity of 470 m/min (rotational speed: 750 rpm); these aligned fibers exhibited nonuniformity in fiber diameter along the fiber axis. The diameters ranged from 200 nm for fine fibers to about 1.3 μm for portions with nonuniformities. These nonuniform portions are composed of MWCNT aggregates as shown in TEM images in Figure 2(a). It was suggested that these aggregates were firmly embedded within the fibers. Despite the stretching force exerted by the rotating disc collector, most of the MWCNT aggregates were unable to disperse themselves as individual tubes. The applied stress was, however, transferred to the elongation and thinning of the portion between the aggregates. The occurrence of stretching could be observed via the reduction in fiber diameter. In the contrast, uniform electrospun PHBV fibers with diameter of 800 nm could be obtained under the same electrospinning condition. Figure 1(c) shows aligned electrospun PHBV fibers collected using disc collector at the same take-up velocity of 470 m/min. Continuous PHBV/MWCNT fibers could not be obtained when the fibers were taken up at a high linear velocity of 940 m/min (or 1500 rpm), indicating that the composite polymeric jets were relatively brittle compared with the pure PHBV jets.

TEM images in Figure 2 show the presence of MWCNTs within the electrospun fibers collected using the rotating disc. Irregular structures consisting of MWCNT aggregates were observed to be protruding from the surfaces of the fibers. From Figure 2(b), a multilayered structure, identified as MWCNT, was observed near the surface of the fiber. The orientation of the MWCNT was parallel to the fiber axis, suggesting that the MWCNT within the polymer matrix aligned itself in the stretch direction during the spinning process. Although dispersion state of MWCNTs within the fibers is unclear, the electrical conductivity measurements performed on a single fiber across gold electrodes, as shown in the later section, indicate that the MWCNTs may be interconnected with one another, forming a network.

### Structural analysis of PHBV fibers collected on stationary plate

Because of the polymorphic nature of PHBV, the polymeric chains are able to develop into α phase, folded chain crystals (molecules in helix conformation) and β phase, extended chain crystals (molecules in planar zig-zag conformation). Tanaka et al.[26] performed enzymatic degradation of PHBV fibers

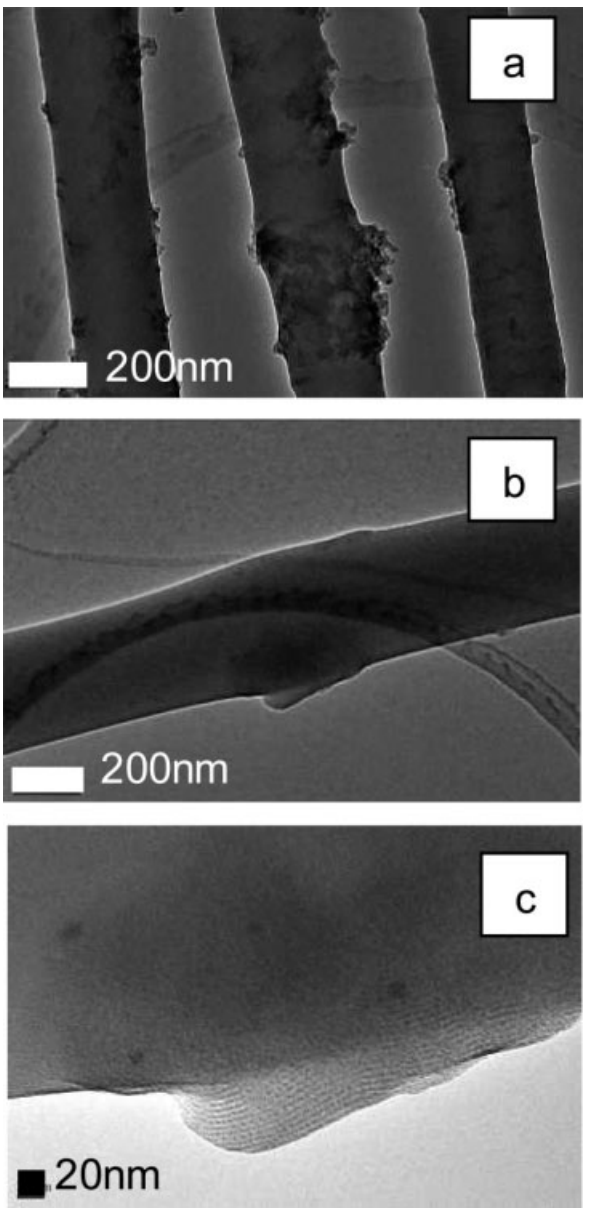


**Figure 2** TEM images showing (a) the presence of MWCNT aggregates found along the surface of aligned electrospun PHBV/MWCNT (0.2 wt %) fiber, (b) MWCNTs found on the surface of electrospun PHBV/MWCNT fiber, and (c) higher magnification of the MWCNT structure embedded within the composite fiber.

composed of α- and β-phase crystals and demonstrated that the α-phase crystals are more resistant to enzymatic degradation compared with the β phase. For applications requiring extended degradation time, such as bone tissue scaffolds, it has been suggested that α-phase crystals would be more desirable. Kim et al.[27] had previously associated the wavenumber 1278 and 1260 $cm^{-1}$ for asymmetrical C—O—C stretching and symmetrical C—O—C with α and β phase, respectively.

Figure 3 shows the FTIR spectra in the range from 1200 to 1800 $cm^{-1}$ for electrospun PHBV fibers and PHBV/MWCNT composite fibers with MWCNT content of 0.2 (0.4), 0.6, and 0.8 wt %, respectively, obtained using stationary flat plate collector. The FTIR spectra of the fiber membranes indicated that at high MWCNT content, a lower intensity of the band of 1260 $cm^{-1}$ associated with β-phase crystal was observed in comparison with the one associated with α phase, implying that the population of α-phase crystals is dominant in the PHBV/MWCNT composite fibers with higher MWCNT content. Effects of MWCNTs on PHBV crystallization were not unexpected as CNTs were reported to exhibit nucleating effects on PHBV, and in this case, the addition of CNTs into electrospun composite fiber still favored the domination of α-phase crystals.[28] An observation to be noted is the FTIR band assigned to carbonyl bond stretching of the crystalline phase. The band shifted from 1718 $cm^{-1}$ for electrospun pure PHBV fibers to 1722 $cm^{-1}$ for electrospun composite fibers with MWCNT content of 0.6 and 0.8 wt %. Such shift to high wavenumbers is associated with the reduction in molecular chain

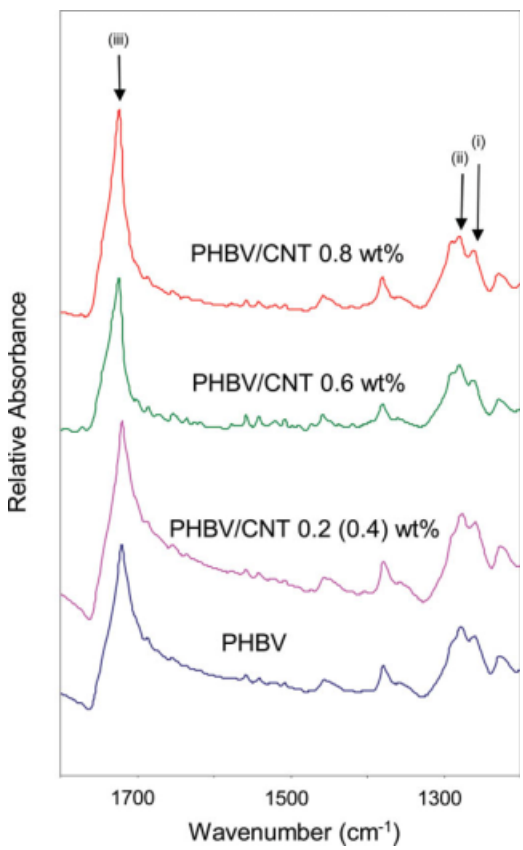


**Figure 3** FTIR spectra for electrospun PHBV incorporated with different content of MWCNT. Symmetrical C—O—C stretching and asymmetrical C—O—C stretching associated with α and β phase, respectively, can be found at 1200 and 1800 $cm^{-1}$ represented by band (i) and (ii). Carbonyl bond stretching is represented by band (iii). [Color figure can be viewed in the online issue, which is available at www.interscience.wiley.com]

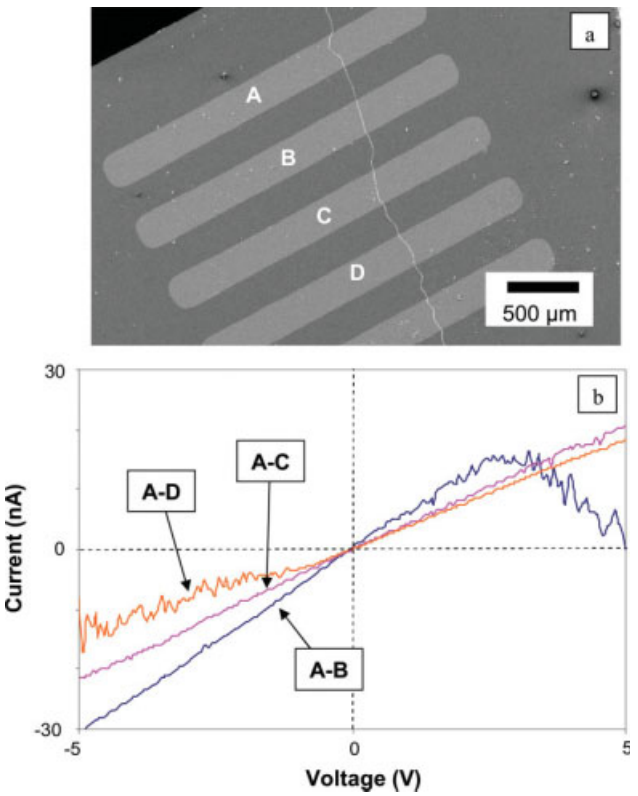


**Figure 4** (a) SEM image of single-electrospun PHBV/MWCNT (0.2 wt %) fiber deposited across a gold electrode. Fiber diameter and length are of 1.2 ± 0.3 μm and about 3000 μm, respectively. (b) Current–voltage curve of single-electrospun PHBV/MWCNT (0.2 wt %) fiber obtained by fixing one of the measuring probes on the first electrode and shifting the other probe to the adjacent electrodes. The label on the respective current–voltage curve indicates the location of the second electrode and the curve obtained during measurement. [Color figure can be viewed in the online issue, which is available at www.interscience.wiley.com]

packing density, and in this case, the obtained spectra suggested that the addition of MWCNT up to 0.6 wt % could induce a change in the polymer's crystalline density.[29]

### Electrical properties of single-electrospun PHBV/MWCNT (0.2 wt %) fiber

A single-electrospun PHBV/MWCNT (0.2 wt %) fiber was obtained across a pair of parallel electrodes fixed on the rotating disc; the fibers were collected using a take-up velocity of 470 m/min. The fiber was placed on indium phosphate substrate with gold electrodes via a masking method. The distance between two adjacent gold electrodes is about 200 μm. Figure 4(a) shows the SEM image of the composite fiber deposited across a few electrodes. The average fiber diameter of about 1.2 ± 0.3 μm with a length of about 3000 μm had been deposited across the substrate. Conductivity measurements were performed across a fiber length of 1400 μm.

Current–voltage (*I–V*) curves were obtained by placing two measuring probes on the gold electrodes, in close contact with the fiber. Fixing one of the probes on an electrode pad, electrical measurement was performed by shifting the other probes to adjacent electrodes. The SEM micrograph of the fiber and the *I–V* curves are shown in Figure 4. To understand the electrical characteristic of the indium phosphate and investigate into the possibility of current leakage via the substrate, a measurement was performed based on one of the probes positioned on the electrode and the other, next to gold electrode, on the indium phosphate surface. *I–V* curve for the measurement can be found in Figure 5(a). From the *I–V* curve, the resistance of indium phosphate was estimated to be in the magnitude of $10^2$ GΩ. To evaluate contact resistance, the curve based on measured resistance plotted against fiber length was obtained,

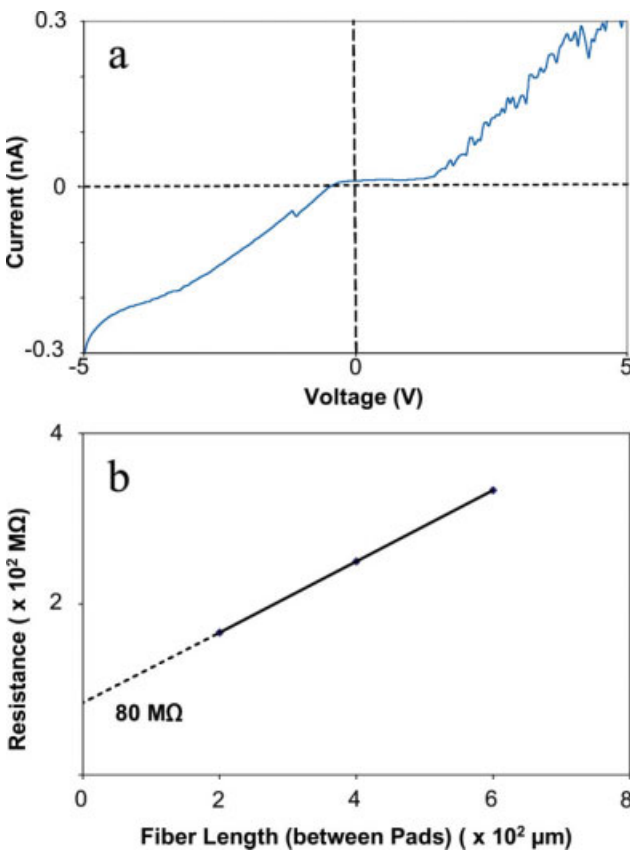


**Figure 5** (a) *I–V* curve obtained when one of the probes is placed on the gold conducting electrode pad and the other, next to the electrode, on the surface of the indium phosphate substrate. (b) The graph of measured resistance plotted against fiber length (between pads), which is used to obtain the value of contact resistance within the system. [Color figure can be viewed in the online issue, which is available at www.interscience.wiley.com]

as seen in Figure 5(b). The values of the resistances were obtained using the linear portions of the *I–V* curves in Figure 4(b). The fiber length, in this case, does not include the portions of the fiber that are in contact with the conducting electrode pads. The point where the curve intersects the vertical axis is the contact resistance value.

After excluding the contact resistance of 80 MΩ, the calculated average conductivity was about 2.07 $Sm^{-1}$. Conductivity values for fiber length of 200 (portion between A–B), 400 (portion between A–C), and 600 μm (portion between A–D) are 2.04, 2.08, and 2.09 $Sm^{-1}$, respectively. It should be highlighted that the presence of electrical conductance within the single fiber over a length of 1400 μm suggests that a continuous and extensive network of interconnected MWCNTs exist within the fiber.

Sundaray et al.[30] obtained similar order of magnitude for conductivity based on single-electrospun PMMA/MWCNT fibers based on two electrodes, neglecting contact resistance in their calculations. In their work, they reported that the conductivity showed an increase of one order from $10^{-3}$ to $10^{-2}$ $Sm^{-1}$ when they increased the content of MWCNT from 0.05 to 2 wt %. The maximum saturated conductivity in their study was found to be $10^{-2}$ $Sm^{-1}$.

## CONCLUSIONS

The morphology and dispersion state of MWCNTs within electrospun PHBV/MWCNT fibers were highlighted in this work. MWCNTs were observed to be dispersed along the surfaces of the electrospun composite fibers collected via a rotating disc collector. FTIR analysis of electrospun fibers deposited on the stationary collector showed that the addition of MWCNT into the PHBV system did not increase the relative content of β-phase crystal within the electrospun fibers. On the other hand, the FTIR also suggested that increasing MWCNT content in electrospun composite fiber could lead to the development of PHBV crystals with lower packing density.

Electrical conductance and contact resistance were obtained via probing of a single-electrospun PHBV composite fiber with low MWCNT content of 0.2 wt %, deposited across multiple electrodes. The calculated conductivity was a remarkable value of about 2.07 $Sm^{-1}$.

## References


1. Reneker, D. H.; Chun, I. Nanotechnology 1996, 7, 216.
2. Bognitzki, M.; Czado, W.; Frese, T.; Schaper, A.; Hellwig, M.; Steinhart, M.; Greiner, A.; Wendorff, J. H. Adv Mater 2001, 13, 70.
3. Dalton, A. B.; Collins, S.; Munoz, E.; Razal, J. M.; Ebron, V. H.; Ferraris, J. P.; Coleman, J. N.; Kim, B. G.; Baughman, R. H. Nature (London) 2003, 6941, 703.
4. Formhals, A. U.S. Pat. 1,975,504 (1934).
5. Inai, R.; Kotaki, M.; Ramakrishna, S. Nanotechology 2005, 16, 208.
6. Iijima, S. Nature (London) 1991, 6348, 56.
7. Tans, S. J.; Devoret, M. H.; Dai, H.; Thess, A.; Smalley, R. E.; Geerligs, L. J.; Dekker, C. Nature 1997, 386, 474.
8. Satio, R.; Fujita, M.; Dresselhaus, G.; Dresselhaus, M. S. Phys Rev Lett B 1992, 46, 1804.
9. Langer, L.; Bayot, V.; Grivei, E.; Issi, J.-P.; Heremans, J. P.; Olk, C. H.; Stockman, L.; Van Haesendonck, C.; Bruynseraede, Y. Phys Rev Lett 1996, 76, 479.
10. Zhao, B.; Hu, H.; Haddon, R. C. Adv Funct Mater 2004, 14, 71.
11. Grunlan, J. C.; Kim, Y. S.; Ziaee, S.; Wei, X.; Abdel-Magid, B.; Tao, K. Macromol Mater Eng 2006, 291, 1035.
12. Mattson, M. P.; Haddon, R. C.; Rao, A. M. J Mol Neurosci 2000, 14, 175.
13. Hu, H.; Ni, Y.; Montana, V.; Haddon, R. C.; Parpura, V. Nano Lett 2004, 4, 507.
14. Zeng, H. L.; Gao, C.; Yan, D. Y. Adv Funct Mater 2006, 16, 812.
15. Huang, S.; Yee, W. A.; Tjiu, W. C.; Liu, Y.; Kotaki, M.; Boey, Y. C. F.; Ma, J.; Liu, T.; Lu, X. Langmuir 2008, 24, 13621.
16. Li, L.; Li, C. Y.; Ni, C.; Rong, L.; Hsiao, B. Polymer 2007, 48, 3452.
17. Valentini, L.; Biagiotti, J.; Kenny, J. M.; Santucci, S. J Appl Polym Sci 2003, 87, 708.
18. Webster, T. J.; Waid, M. C.; McKenzie, J. L.; Price, R.; Ejiofor, J. U. Nanotechnology 2004, 15, 48.
19. Supronowicz, P. R.; Ajayan, P. M.; Ullmann, K. R.; Arulanandam, B. P.; Metzger, D. W.; Bizios, R. J Biomed Mater Res 2002, 59, 499.
20. Dror, Y.; Salalha, W.; Khalfin, R. L.; Cohen, Y.; Yarin, A. L.; Zussman, E. Langmuir 2003, 19, 7012.
21. Ko, F.; Gogotsi, Y.; Ali, A.; Naguib, N.; Ye, H.; Yang, G.; Li, C.; Willis, P. Adv Mater 2003, 15, 1161.
22. Correa-Duarte, M. A.; Wagner, N.; Rojas-Chapana, J.; Morsczeck, C.; Thie, M.; Giersig, M. Nano Lett 2004, 4, 2233.
23. Ojha, S. S.; Stano, D. R. S. K.; Hoffman, T.; Clarke, L. I.; Gorga, R. E. Macromolecules 2008, 41, 2509.
24. Yee, W. A.; Kotaki, M.; Liu, Y.; Lu, X. Polymer 2007, 48, 512.
25. Eitan, A.; Jiang, K. Y.; Dukes, D.; Andrews, R.; Schadler, L. S. Chem Mater 2003, 15, 3198.
26. Tanaka, T.; Yabe, T.; Teramachi, S.; Iwata, T. Polym Degrad Stab 2007, 92, 1016.
27. Kim, G. M.; Michler, G. H.; Radusch, H. J.; Wutzler, A. J Appl Polym Sci 2006, 103, 860.
28. Lai, M.; Li, J.; Yang, J.; Liu, J.; Tong, X.; Cheng, H. Polym Int 2004, 53, 1479.
29. Lee, K. H.; Kim, K. W.; Pesapane, A.; Kim, H. Y.; Rabolt, J. F. Macromolecules 2008, 41, 1494.
30. Sundaray, B.; Subramanian, V.; Natarajan, T. S.; Krisnamurthy, K. Appl Phys Lett 2006, 88, 143114-1.